REGENERATION MECHANISM OF ORGANIZED STRUCTURES IN NEAR-WALL TURBULENCE

M. F. Baig and S. I. Chernyshenko
AFM, School of Engineering Sciences
University of Southampton, Southampton SO17 1BJ, UK
e-mail: M.F.Baig@soton.ac.uk, S.Chernyshenko@soton.ac.uk

ABSTRACT

A direct numerical simulation of quasi-2D (that is with flow parameters independent of longitudinal coordinate) decaying and forced turbulence and 3D turbulence in channel flow was performed with the intention of ascertaining the sustenance mechanism of near-wall turbulence by investigating the mechanism of streak formation. We found the existence of streaks in quasi-2D flows thus demonstrating that contrary to many theories, feedback from longitudinal flow is not necessary for streak formation. Passive scalars having different mean scalar profiles were introduced in forced quasi-2D and 3D turbulent flows in order to compare the streak spacing of the scalars deduced from two-point correlations of DNS results with results obtained theoretically. It has been found that even for the same vortex structure for all the passive scalars there is a marked variation in streak spacing implying that the preferential streak spacing is not necessarily linked to the preferential vortex spacing. The obtained qualitative numerical results are in favour of the theory of streak formation based on optimal perturbation (Butler and Farrel 1993) but at the same time they clearly indicate that the good quantitative agreement reported for that theory may be fortuitous.

INTRODUCTION

The near-wall turbulence is dominated by organized structures of two types, namely quasi-streamwise vortices and streaks. The streaks are primarily alternating high and low-speed streamwise jets having an average spanwise wavelength of 100 wall units (Smith and Metzler, 1983). The quasi-streamwise vortices are roughly 200 wall units long (Robinson, 1991) and merge into disorganised vorticity after leaving the immediate wall neighbourhood. Near-wall turbulence is sustained through a continuous generation and break-down of these coherent structures which also leads to development of turbulent wall-drag.

For turbulence to sustain itself, vortices must recur. Numerous regeneration mechanisms have been proposed involving either the self-reproduction of existing vortices (parent-offspring scenario) or the instability of a quasi-steady base flow. In the 'parent-offspring' scenario according to Smith and Walker (1994) new vortices are generated by direct induction near the existing spanwise arch and legs of the parent vortex. Jimenez and Orlandi (1993) attribute vortex formation to 2D Kelvin-Helmholtz type of roll-up of near-wall streamwise vorticity sheets. Where an instability is assumed to be the primary mechanism of streak formation, there is a considerable disagreement regarding its nature. Majority of the existing theories are essentially three-dimensional. This includes all the parent-offspring scenarios and the instability-based theories including direct resonance of oblique modes (Jang et. al., 1986), centrifugal instability (Sreenivasan, 1988), shear-driven instability (Hamilton et. al., 1995), and streak instability without any parent vortex (Schoppa and Hussain, 1998).

There are two instability-related theories, however, where the streaks are formed from a non-organised background even if the dependence of the flow parameters on the longitudinal coordinate is absent. One is the optimal perturbation theory (Butler and Farrell, 1993) which is based on the linearized Navier-Stokes equations. This theory seeks a perturbation to the mean turbulent velocity profile such that its energy grows to a maximum possible value over the so-called eddy turnover time equal to $\tau_e = q^2/\epsilon$, the ratio of the square of the characteristic turbulent kinetic energy, $q^2 = \overline{u_i u_i}$, to the dissipation rate $\epsilon = \nu \overline{u_{i,j} u_{i,j}}$. It is assumed that in this time the streaks are destroyed by the chaotic motion. The optimum perturbations turn out to consist of longitudinal vortices creating the streaks by the lift-up mechanism. The other theory (Nikitin and Chernyshenko, 1997) explains the formation of longitudinal vortices as a result of instability caused by Reynolds normal stress anisotropy. In near-wall turbulent flows the difference $Q = < v'^2 - w'^2 >$ between wall-normal and lateral Reynolds normal stresses is non-zero. Longitudinal vortices can advect Q and the non-uniformity in Q, in turn, can generate fluid motion. It turns out that in turbulent flow the distribution of Q is such that vortices can grow. On the whole this process is similar to the Rayleigh-Benard instability in a fluid layer heated from below, with the derivative of Q in wall-normal direction playing the role of the buoyancy force. Both theories, when applied to a usual turbulent near-wall flow, predict the correct streak spacing. Both theories use empirical data, the Q distribution for the Nikitin and Chernyshenko (1997) theory and mean velocity and eddy turnover time distribution for the Butler and Farrel (1993) theory. For brevity we will use the abbreviations RNSAI (Reynolds-Normal-Stress-Anisotropy-induced Instability theory) and OP (Optimal Perturbation theory).

It is generally agreed that streaks appear due to wall-normal motions of the fluid. Such motions create streaks by carrying the slowly-moving fluid away from the wall. In a pure form this mechanism is illustrated in Fig.1. This picture implies that the streak spacing is determined by and is equal to the vortices spacing. Accordingly, all theories except the OP theory predict in fact the dominant vortex spacing and assume the streak spacing to be twice of the same. In the OP theory, however, the optimal vortices are just the vortices which are the most efficient in generating streaks. While the energy of the optimal streaks grow, the energy of the optimal vortices decays monotonically. There-

This study is supported by EPSRC under Grant GR/R27785/01

fore, there is no reason to expect that these vortices will dominate the flow. This fact, while present in the optimal solutions, seems to have not yet been recognised.

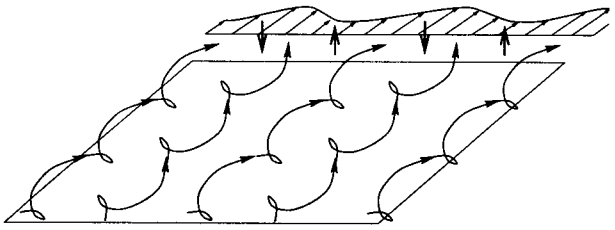

Figure 1: Lift-up mechanism of streak formation

The present study aims at checking the various theories of streak generation. Three sets of numerical experiments were performed. In the first and the second set of calculations we consider flows independent of longitudinal coordinate. This eliminates all theories that rely on three-dimensionality of the flow, leaving only RNSAI and OP theories. To distinguish between them, we prescribe random initial conditions with spanwise length scales within a certain range. Within OP, which is linear, no streaks with spanwise wavelength outside that range can appear. We also vary the amplitude of the initial conditions. This does not affect OP but according to RNSAI, which is non-linear since the Reynolds normal stresses are non-linear, the instability can appear only if the amplitude is high enough, so that no streaks should be observed when the amplitude is below a certain threshold value. In the first set we allow the cross-flow motion to decay naturally, while in the second set a random body force is introduced and the statistically steady state is analysed. In the third set the limitation of zero derivatives in the flow direction is dropped, and body forces are again assumed to be zero. Full DNS of turbulent flow is performed. In the last two sets of numerical experiments we introduce passive scalars with different mean distributions in the wall-normal direction. Streaks in the passive admixture concentration are expected to be formed by the same lift-up mechanism. Naturally, the vortex structure is the same for all passive scalars but OP predicts variation in the streak spacing as a result of the variation in the mean admixture concentration profile. We compare the streak spacing in the passive admixture obtained in calculations with predictions of RNSAI and OP theories.

QUASI-2D DECAYING TURBULENCE

Initial conditions of mean turbulent streamwise velocity profile with no perturbations and random cross-flow velocity perturbations have been considered. The initial conditions and, hence, the entire solution are independent of the longitudinal coordinate, x. Since $\partial/\partial x = 0$, the continuity and momentum equations take the form (with f_x, f_y and f_z, for a while, being zero):

$$\frac{\partial v}{\partial y} + \frac{\partial w}{\partial z} = 0 \qquad (1)$$

$$\frac{\partial u}{\partial t} + v\frac{\partial u}{\partial y} + w\frac{\partial u}{\partial z} = -\frac{\partial p}{\partial x} + \frac{1}{Re}\nabla^2 u + f_x \qquad (2)$$

$$\frac{\partial v}{\partial t} + v\frac{\partial v}{\partial y} + w\frac{\partial v}{\partial z} = -\frac{\partial p}{\partial y} + \frac{1}{Re}\nabla^2 v + f_y \qquad (3)$$

$$\frac{\partial w}{\partial t} + v\frac{\partial w}{\partial y} + w\frac{\partial w}{\partial z} = -\frac{\partial p}{\partial z} + \frac{1}{Re}\nabla^2 w + f_z \qquad (4)$$

where $\partial p/\partial x$ = -1. The boundary conditions are no-slip for the walls, i.e. $\mathbf{u} = 0$, and periodicity in spanwise and streamwise directions. From the equations (1)-(4) it can be seen that the cross-flow equations do not involve the longitudinal velocity u, that is v and w are governed by the 2D continuity and Navier-Stokes equations (1), (3) and (4). For the initial conditions, a random eddy model has been constructed, in which the streamwise component u is given by mean turbulent streamwise velocity profile with no perturbations, while v and w are

$$v(y,z) = -A\sum_{i=1}^{N}(-1)^i \frac{(z-z_i)}{a_i^2} h(\tilde{r}) \qquad (5)$$

$$w(y,z) = A\sum_{i=1}^{N}(-1)^i \frac{(y-y_i)}{a_i^2} h(\tilde{r}) \qquad (6)$$

where A is the amplitude by which we can increase or decrease the magnitude of the random velocity perturbations, N is the number of generated random eddies, y_i and z_i are the coordinates of the center of the eddies, and $\tilde{r}$ and $h(\tilde{r})$ are given by

$$\tilde{r} = \sqrt{\frac{(z-z_i)^2}{a_i^2} + \frac{(y-y_i)^2}{a_i^2}} \qquad (7)$$

$$h(\tilde{r}) = 0, \quad \tilde{r} \geq 1$$

$$h(\tilde{r}) = e^{(\tilde{r}-1)^{-2}}, \quad \tilde{r} \leq 1$$

In order to have a homogeneous random distribution of eddies in the spanwise direction, we assume $y_i = f(\zeta,\eta) = L_y\zeta$ where L_y is the length in spanwise direction and ζ are the random numbers generated based on uniform deviates which lie within a range of (0 to 1). Similarly, a non-homogeneous random distribution of eddies in wall-normal direction is achieved using $z_i = g(\zeta,\eta) = cos(\pi\eta)$, where η are the random numbers based on uniform deviates which also lie within a range of (0 to 1). This gives a larger concentration of eddies near the walls at $z = \pm 1$. The probability density function (PDF) $\rho(y,z)$ governing the distribution of random eddies in two-dimensional space is given by the relation (Panchev, 1971)

$$\rho(y,z) = \tilde{\rho}(\zeta,\eta)J^{-1} = \frac{1}{L_y f(\eta)} = \frac{1}{L_y \pi sin(\pi\eta)} \qquad (8)$$

where J is the Jacobian $\begin{vmatrix} g_\zeta & g_\eta \\ f_\zeta & f_\eta \end{vmatrix}$. This shows that the PDF of eddy distribution peaks near the walls z=±1.

From the definition of number density, we can relate the mean distance l between the centers of randomly distributed eddies to the number of randomly generated eddies N and the PDF $\rho(y,z)$ as

$$l = \frac{K}{\sqrt{(\rho(y_i,z_i)N}} \qquad (9)$$

where K is a constant. We took $a_i = l(y_i,z_i)$. The eddies which overlap with the walls are excluded, i.e. if $|z_i - 1| \leq a_i$ or $|z_i + 1| \leq a_i$, we ignore that eddy.

Formation of streamwise streaks

The numerical experiments have been performed in a computational box of size L_x =0.005, L_y=6.0 and L_z = 2.0 on a grid having 4*480*480 nodal points at a Re_τ=180.0 using a pseudo-spectral parallel code of Sandham and Howard (1998) on Linux Beowulf cluster. The Fourier transform was

performed on the velocity field (5,6), and modes corresponding to highest and lowest fifty wave-numbers were excluded. The resulting flow field did not contain any wavelength above 0.1 and was used as the initial condition. The simulations have been performed for a maximum non-dimensional time of 0.4 at a constant amplitude $A = 4.0$ and $N = 5000$ eddies corresponding to a initial cross-flow Reynolds number $Re_{cf} = 305$ based on mean kinetic cross-flow velocity. The temporal development of the streaks can be seen from the fluctuating negative streamwise velocity contours as shown in Fig.2, corresponding to non-dimensional times 0.05 and 0.4. At $t = 0.4$, the streak spacing is outside the range of the wavelengths present in the initial conditions. The evolution of the power spectrum was analysed. The total cross-flow perturbation energy quickly decreases, but there is transient energy growth in the large-wavelength part of the spectrum. This, of course, is the well-known inverse energy cascade. However, at the initial stages no wavelength selection was observed. One should note, however, that this initial stage was only marginally resolved in our calculations. Calculations were made with different amplitudes of the initial velocity perturbation. We did observe disappearance of streaks where the amplitude was small, however, the threshold value was so small that the influence of rounding errors cannot be eliminated. The profiles of the difference in cross-flow normal Reynolds stresses was also calculated. It indeed exhibit a behaviour which can lead to a transient RNSAI, but since the mean flow is time-dependent, no direct comparison with this theory could be made. The observed streak spacing increases with time. Figure 3 shows a comparison of the number of streaks as a function of time as predicted by optimal perturbations (the data from Fig.3 in (Butler and Farrel, 1993)) with the number of streaks observed in our calculations. Therefore, the observed behaviour can be described as an initial non-linear inverse energy cascade in the cross-flow, followed by a decay described by linearized equations. The decaying cross-flow perturbations then form the longitudinal streaks via the mechanism described by the optimal perturbation theory. At this stage it remains unclear whether the dominance of the linear OP mechanism is not simply due to the small amplitude of the initial perturbations. However, we could not increase the initial amplitude because of the limited computer resources available.

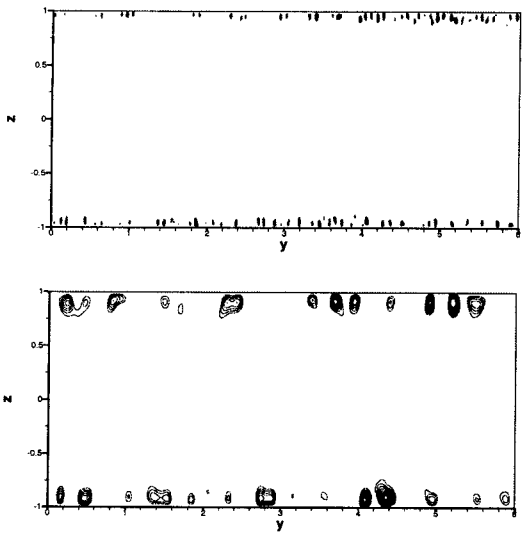

Figure 2: Streamwise velocity u' at time instants t=0.05 (top) and t=0.4 .

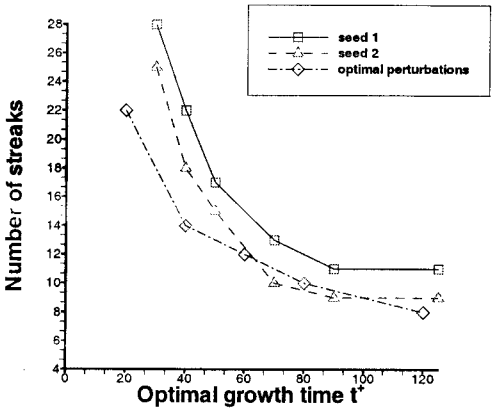

Figure 3: Comparison of number of streaks for two different realisations of decaying quasi-2D turbulence with streaks computed based on optimal perturbation theory. Seeds 1 and 2 refer to two different sets of initial conditions.

PASSIVE SCALAR ADMIXTURE STREAKS

Passive scalar admixture concentration θ is governed by the equation

$$\frac{\partial \theta}{\partial t} + v\frac{\partial \theta}{\partial y} + w\frac{\partial \theta}{\partial z} = S + \frac{1}{RePr}\nabla^2\theta \qquad (10)$$

where $S(z)$ is the source term for the passive scalar. Provided that the mean profile of θ is similar to the mean profile of the longitudinal velocity, the same lift-up mechanism illustrated in Fig 1 which produces the velocity streaks, produces also 'admixture streaks', that is regions where θ is smaller than average. This allows to isolate the influence of the shape of the mean profile on the streak spacing. Calculations with different mean admixture profiles can be performed simultaneously, and all of them will have exactly the same vortex structure. We have modified the pseudo-spectral channel code of Sandham and Howard (1998), in order to solve an arbitrary number of passive-scalar equations.

Streaks are not exactly regular, and different definitions of streak spacing are possible. The velocity auto-correlation function $R_{uu}(\Delta, z) = \langle u(t,x,y,z)u(t,x,y+\Delta,z)\rangle$ has a maximum at $\Delta = 0$ and reaches a minimum at a certain value $\Delta_{\min}$. For brevity, we omit the argument z in the following formulae. Streak spacing can be defined as $2\Delta_{\min}$. Similarly, the auto-correlation function for the passive admixture concentration can be used for determining the admixture streak spacing.

Since the equations for the admixture concentration are linear, a linear combination of several solutions is a solution. If $\theta = \sum_{i=1}^{i=n} A_i\theta_i$ then

$$R_{\theta\theta}(\Delta) = \sum_{i=1,j=1}^{i=n,j=n} A_i A_j R_{\theta_i\theta_j}(\Delta)$$

Note that the averaged profile of the admixture concentration is

$$\bar{\theta} = \langle\theta\rangle = \sum_{i=1}^{i=n} A_i\langle\theta_i\rangle = \sum_{i=1}^{i=n} A_i\bar{\theta}_i.$$

Therefore, by solving simultaneously several passive-admixture equations with different source terms and calcu-

lating the cross-correlations $R_{\theta_i\theta_j}(\Delta)$ it is then quite easy to calculate the auto-correlation function and, hence, the streak spacing, for any linear combination determined by the vector of coefficients A_i. Such calculations were performed both in 2D randomly forced flow and in 3D flow. To check the concept, one of the calculated admixture concentrations was a linear combination, so that its auto-correlation function was calculated both directly and by the method described above, and the results coincided. We also compared the streak spacing as calculated from the auto-correlation function with the streak spacing as it, although rather approximately, was obtained from visualisation, and again found that our linear-combination approach works.

For checking to which extent the streak spacing can be varied by varying the mean admixture profile, the following method was used. We sought for such a vector $(A_1, \ldots, A_n)$ of unit length that the corresponding auto-correlation function is as small as possible at the specific value of $\Delta = \Delta_0$. This leads to a minimisation problem for the functional

$$\sum_{i=1,j=1}^{i=n,j=n} A_i A_j [R_{\theta_i\theta_j}(\Delta_0) - \lambda\delta_{i,j}] \rightarrow \min$$

were λ is the Lagrange multiplier and δ_{ij} is the Kronecker delta. This, in turn, can in a standard way be reduced to a linear eigenvalue problem. This method was used both in 2D randomly forced and in 3D flow cases to obtain passive-admixture solutions with quite large and quite small streak spacing. Naturally, for linear combinations obtained in this way, the minimum of the auto-correlation function does not exactly coincide with Δ_0, but in practise Δ_0 and $\Delta_{\min}$ turn out to be close within a reasonable range of Δ_0.

Six basic admixture mean profiles were calculated. For completeness, the best choice of the basic profiles would be a sufficiently large number of Chebyshev polynomials, so that practically any mean profile could be represented as a linear combination of them. However, the required computer resources would be too large. So, we compromise by taking three profiles of the shape more or less close to what seemed to be of possible interest and three other profiles as trigonometric functions. The profiles we used were defined via its derivatives with respect to z, because this derivative is needed for OP theory. Introducing two auxiliary functions,

$$\begin{aligned} g(z, Re) &= 0.5(1 + (0.525\frac{Re}{3}(1 + z^2 - 2z^4) \\ &\quad (1 - e^{(-(1-|z|)\frac{Re}{37})})^2)^{0.5} - 0.5 \end{aligned}$$

($g(z, Re)$ has been used to generate Reynolds-Tiederman profile, as in Waleffe and Kim (1991)), and

$$h(z, d, w) = 150(e^{(-\frac{(-1+d-z)^2}{w^2})} - e^{(-\frac{(-1+d+z)^2}{w^2})}),$$

the derivatives of the basic mean profiles are

$$\begin{aligned} \bar{\theta_1}' &= -z \times Re/(1 + g(z)) \\ \bar{\theta_2}' &= h(z, 0.20, 0.150) \\ \bar{\theta_3}' &= h(z, 0.10, 0.075) \\ \bar{\theta_4}' &= \sin(1 \times \pi(1 + z)/2) \\ \bar{\theta_5}' &= \sin(3 \times \pi(1 + z)/2) \\ \bar{\theta_6}' &= \sin(5 \times \pi(1 + z)/2) \end{aligned}$$

Figure 4 shows the statistically averaged wall-normal variation of mean scalar profiles $\bar{\theta_1}$ to $\bar{\theta_6}$.

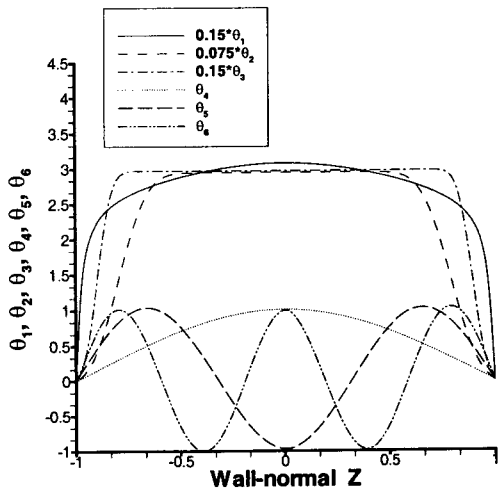

Figure 4: Statistically averaged wall-normal variation of mean scalar profiles $\overline{\theta_i}$

In order to be able to perform comparisons with OP and RNSAI theories, we also developed a set of computer codes for calculating the streak spacing for given Q distribution according to the RNSAI theory and the streak spacing for given mean profile and eddy turnover time according to OP theory. In the latter case the optimal perturbations were assumed to be independent of the longitudinal coordinate, which is, anyway, correct. These codes were verified by reproducing the results from the corresponding papers and then used for the forced 2D and natural 3D cases considered below.

QUASI-2D FORCED TURBULENCE

The numerical experiments were carried out by subjecting quasi-2D turbulent flows to statistically steady-state forcing using random amplitude body force terms (Tsinober, 2001) in the governing Navier-Stokes equations. The initial conditions are the same as mentioned above for quasi-2D decaying turbulence.

The body forces f_y and f_z in eqns. (1)-(4) have random amplitude in time with zero mean, a sinusoidal spatial variation of fixed wavenumbers (l,k) in spanwise and wall-normal directions and a peaked near-wall amplitude in wall-normal direction $\zeta(z)$. In order to generate peaked near-wall forcing which reduces to zero toward the centre of the channel, various functions $\zeta(z)$ have been used ranging from Dirac delta to two-hump functions. The forces are then given as

$$\begin{aligned} f_x &= 0.0 \\ f_z &= A(\omega_f t)\cos(\frac{2\pi ly}{L_y})\zeta(z)\cos(\frac{2\pi kz}{L_z}) \\ f_y &= \frac{0.5A(\omega_f t)(z - z_o)n^2 L_y \sin(\frac{2\pi ly}{L_y})\zeta(z)\cos(\frac{2\pi kz}{L_z})}{\pi l} \\ &\quad + \frac{A(\omega_f t)kL_y \sin(\frac{2\pi kz}{L_z})\zeta(z)\sin(\frac{2\pi ly}{L_y})}{L_z l} \end{aligned} \quad (11)$$

on using divergence-free body force condition. Here $\zeta(z)$ approximates a Dirac delta function centered at z_o with its width controlled by a factor n and is given mathematically as

$$\zeta(z) = e^{(-0.5n^2(z-z_o)^2)}$$

The results presented below were obtained numerically at Re =360 on a 4×256×160 mesh for wall-normal Dirac delta

function having $z_o = 0.95$ and $n = 20$ with a fixed spanwise wavenumber l= 55, wall-normal wavenumber k=1, amplitude $A = 0.05$ and a forcing frequency $\omega_f = 100$ in terms of non-dimensional time. The forcing of the flow leads to fully-developed turbulence by the time $t = 25.0$. The flag is then turned on to perform statistical averaging and the statistics is gathered for a very long time till $t = 330.0$.

The most noticeable feature of this calculation is the presence of the inverse energy cascade. Even though the forcing length scales are small, the energy of long-wave modes is quite high, thus making it difficult to obtain the distribution of Q similar to that observed in real flows. By adjusting the forcing profile $\zeta(z)$ we achieved reasonably good behaviour of Q near the walls, where the streaks are formed, but it remained, in contrast to natural 3D flows, far from zero in the center of the channel. When RNSAI theory calculations were performed we had to ignore the central part of the obtained Q profile. The original (averaged) Q profile and the profile used for RNSAI calculations are shown in Figure 5.

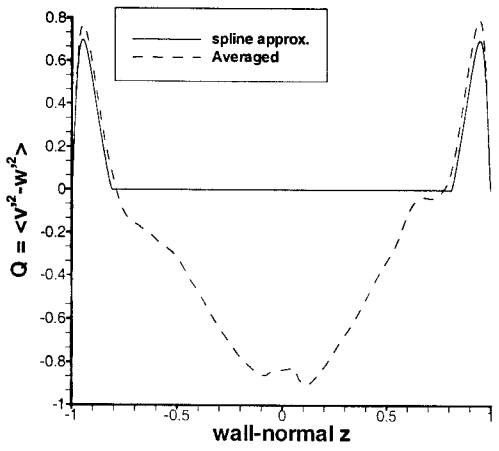

Figure 5: Statistically averaged and spline-interpolated Q vs z profiles

We then used the technique described above to obtain linear combinations of the passive admixture solutions with considerable variation of the streak spacing. For each of these admixture solutions, which we denote $\theta_{n1}, \ldots, \theta_{n5}$, OP theory was applied and the streak spacing calculated. The results are summarised in the following table.

Scalars	Streak spacing, normal units		
	DNS	RNSA	OP
θ_{n1}	0.25	0.86	0.33
θ_{n2}	0.59	0.86	0.55
θ_{n3}	1.30	0.86	0.61
θ_{n4}	2.62	0.86	0.78
θ_{n5}	4.21	0.86	0.97

Table 1: Comparison of streak spacing of scalars θ_{ni} from DNS results of two-point correlations of randomly forced 2D turbulence, from RNSA and OP theories.

3D TURBULENT CHANNEL FLOW

For the third set of experiments, numerical simulations were performed in a periodic channel of $L_x = 6$, $L_y = 3$ and $L_z = 2$ at Re =360 using 128×128×160 mesh with the passive scalars. Starting from a base laminar flow with random perturbations, a fully-developed turbulent flow evolves by the non-dimensional time $t = 12.0$. The flag is then turned on to perform statistical averaging and the statistics is gathered till time $t = 34.0$. The averaged profiles and statistics are in a good agreement with available data. The cross-correlation functions were calculated and then used to build linear combinations of the basic solutions (which were taken to be the same as in the 2D randomly-forced case) with significant variation of the streak spacing. The mean passive admixture profiles of these linear combinations, which we denote $\theta_{3D1}, \ldots, \theta_{3D5}$, are presented in Figure 6.

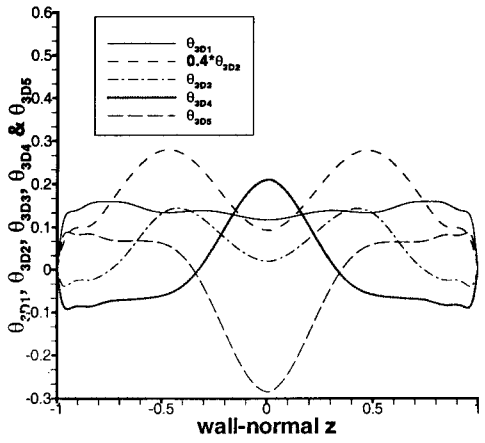

Figure 6: Mean profiles $\overline{\theta_{3Di}}$.

Calculation were then performed using the RNSAI and OP theory, and the results are presented in the Table 2. All the data correspond to the distance to the wall $z = 0.01$. However, it turns out that reliable calculation of the auto-correlations functions for profiles in Figure 6 require noticeably greater averaging period than the averaged period required for the basic profiles. For this reason the values in the DNS column of Table 2, related to the profiles $\theta_{3D1}, \ldots, \theta_{3D5}$, should be considered as preliminary estimates.

Scalars	Streak spacing, wall units		
	DNS	RNSA	OP
θ_1	115	140	100
θ_2	560	140	230
θ_3	500	140	150
θ_4	600	140	420
θ_5	520	140	500
θ_{3D1}	216	140	535
θ_{3D2}	540	140	595
θ_{3D3}	605	140	840
θ_{3D4}	1080	140	720
θ_{3D5}	1080	140	660

Table 2: Comparison of streak spacing obtained from DNS, RNSA and OP for 3D turbulent channel flow.

Note the major point of our results, both in 2D and 3D, namely, strong variation of the streak spacing with variation in the mean scalar profile, while the vortex structure remains the same.

CONCLUSIONS

- Streaks can form in case when all flow parameters are

independent of the longitudinal coordinate. This is the condition at which there is no feedback from the longitudinal flow profile, including the streaks, to the cross-flow vortex structure.

- The streak spacing strongly depends on the mean profile even when the vortex structure is fixed. Theories which assume the streak spacing being equal to twice the vortex spacing, like, for example, RNSA theory by Nikitin and Chernyshenko (1997), cannot explain this fact. The only existing theory which describes similar qualitative behaviour is the OP theory by Butler and Farrell (1993).

- In many cases the streak spacing obtained with the optimal perturbation theory differs considerably from DNS results. Therefore, the good agreement between the quantitative prediction of this theory and streak spacing in the case, when the mean profile coincides with the mean velocity profile, may be fortuitous.

REFERENCES

Butler K.M. and Farrell B.F., 1993, "Optimal perturbations and streak spacing in wall-bounded turbulent shear flows", *Phys. of Fluids* A,5 pp. 774-777.

Hamilton J.M., Kim J. and Waleffe F., 1995, "Regeneration mechanisms of near-wall turbulence structures", *J. Fluid Mech.*, Vol. 232, pp. 317-348.

Henningson D. and Schmidt P., 2000, *Stability analysis of Shear flows*, Springer Verlag, Berlin, 2000.

Jang P. S., Benney D. J. and Gran R.L, 1986, "On the origin of streamwise vortices in a turbulent boundary layer", *J. Fluid Mech.*, Vol. 169, pp. 109-123.

Jimenez, J. and Orlandi, P., 1993, "The rollup of vortex layer near a wall", *J. Fluid Mech.*, Vol. 248, pp. 297.

Kim J., Moin P. and Moser R., 1987, "Turbulence statistics in fully developed channel flow at low Reynolds number", *J. Fluid Mech.*, Vol. 177, pp. 133-166.

Nikitin N. and Chernyshenko S., 1997, "On the nature of organised structures in turbulent near-wall flows", *Fluid Dynamics*, Vol. 32(1), pp. 18-23.

Panchev S. 1971, *Random functions and Turbulence*, Pergamon Press, New York.

Panton R., 1997, *Self-sustaining mechanism of wall-turbulence*, Editor, Computational Mechanics Publication, Southampton.

Press W., Teukolsky S., Vellerling W. and Flannery B., 1992, *Numerical Recipes in Fortran*, Cambridge University Press, Cambridge.

Robinson S., 1991, "Coherent motions in the turbulent boundary layer", *Ann. Rev. Fluid Mech.*, Vol. 23, pp.601-639.

Sandham N. and Howard R., 1998, "Direct simulation of turbulence using massively parallel computers", *Parallel Computational Fluid Dynamics*, Editors D. Emerson et. al., North-Holland.

Schoppa W. and Hussain A., 1998, "Formation of near-wall streamwise vortices by streak instability", AIAA 98-3000, *29th AIAA Fluid dynamics Conf.*, Albuquerque, USA.

Smith, C. and Metzler, S., 1983, "The characteristics of low-speed streaks in the near-wall region of a turbulent boundary layer", *J. Fluid Mech.*, Vol. 129, pp. 27-54.

Smith, C.R. and Walker, J.D.A., 1994, "Turbulent wall layer vortices", *Fluid Vortices*, Ed. S. Green, Springer-Verlag.

Sreenivasan, K, 1988, "A unified view of the origin and morphology of the turbulent boundary layer structure", *Proc. IUTAM Symp. on Turbulence Management and Relaminarisation*, Ed. Liepmann H and Narasimha R., pp. 37-61, Springer.

Tsinober A., 2001, *An informal introduction to turbulence*, Kluwer Publishers.

Waleffe, F. and Kim, J., 1991, "On the origin of streaks in turbulent shear flows", *8th Symposium on Turbulent shear flows*, pp. 5-5, Springer-Verlag.